International Tables for Crystallography (2006). Vol. F, Chapter 6.1, pp. 125–132.

6. RADIATION SOURCES AND OPTICS

6.1. X-ray sources

BY U. W. ARNDT

6.1.1. Overview

In this chapter we shall discuss the production of the most suitable X-ray beams for data collection from single crystals of macromolecules. This subject covers the generation of X-rays and the conditioning or selection of the X-ray beam that falls on the sample with regard to intensity, cross section, degree of parallelism and spectral composition. The conclusions drawn do not necessarily apply to smaller-unit-cell crystals or to noncrystalline samples.

6.1.2. Generation of X-rays

X-rays are generated by the interaction of charged particles with an electromagnetic field. There are four sources of interest to the crystallographer.

(1) The bombardment of a target by electrons in a vacuum tube produces a continuous ('white') X-ray spectrum, called *Bremsstrahlung*, which is accompanied by a number of discrete spectral lines characteristic of the target material. The most common target material is copper, and the most frequently employed X-ray line is the copper $K\alpha$ doublet with a mean wavelength of 1.542 Å. X-ray tubes are described in some detail in Chapter 4.2 of *IT* C (1999). We shall consider only the most important points in X-ray tube design here.

(2) Synchrotron radiation is produced by relativistic electrons in orbital motion. This is the subject of Part 8.

(3) The decay of natural or artificial radioisotopes is often accompanied by the emission of X-rays. Radioactive sources are often used for the testing and calibration of X-ray detectors. For our purposes, the most important source is made from ^{55}Fe, which has a half-life of 2.6 years and produces Mn $K\alpha$ X-rays with an energy of 5.90 keV.

(4) Ultra-short pulses of X-rays are generated in plasmas produced by the bombardment of targets by high-intensity subpicosecond laser pulses (*e.g.* Forsyth & Frankel, 1984). In earlier work, the maximum pulse repetition frequency was much less than 1 Hz, but picosecond pulses at more than 1 Hz are now being achieved with μm-size sources. The time-averaged X-ray intensities from these sources are very low, so their application will probably remain limited to time-resolved studies (Kleffer *et al.*, 1993).

X-rays also arise in the form of channelling radiation resulting from the bombardment of crystals, such as diamonds, by electrons with energies of several MeV from a linear accelerator (Genz *et al.*, 1990) and in the form of transition radiation when multiple-foil targets are bombarded by electrons in the range 100–500 MeV (*e.g.* Piestrup *et al.*, 1991). It will be some time before these new sources can compete with the older methods for routine data collection.

6.1.2.1. *Stationary-target X-ray tubes*

A section through a permanently evacuated, sealed X-ray tube is shown in Fig. 6.1.2.1 The tube has a spirally wound tungsten filament, F, placed immediately behind a slot in the focusing cup, C, and a water-cooled target or anode, T, approximately 10 mm from the surface of C. The filament–focusing-cup assembly is at a negative voltage of between 30 and 50 kV, and the target is at ground potential. The electron beam strikes the target in a focal line,

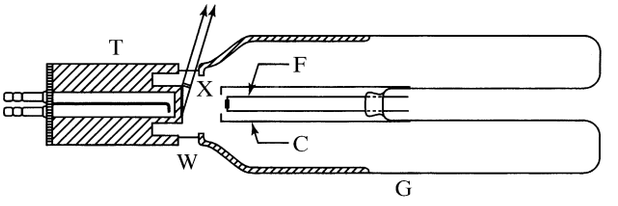

Fig. 6.1.2.1. Section through a sealed X-ray tube. G, glass envelope; F, filament leads (at negative high voltage); C, focusing cup; T, target (at ground potential); W, one of four beryllium windows. The electron beam forms a line on the target, which is viewed at a small take-off angle to form a foreshortened effective source X.

which acts as a line source of X-rays. There are usually two pairs of X-ray windows, W, through which the source is viewed at a small angle to the target surface, thus producing a foreshortened effective source, X, which is approximately square in one plane and a narrow line in the other. Focus dimensions on the target and maximum recommended power loading are shown for a number of standard inserts in Table 6.1.2.1. None of these are ideal for macromolecular crystallography. The assembly of a cathode, anode and windows – the tube insert – is inserted in a shock- and radiation-proof shield which is fixed to the table. Attached to the shield are X-ray shutters and filters, and sometimes brackets for bolting on X-ray cameras. A high-voltage connection is made to the tube by means of a flexible, shielded, shock-proof cable; nowadays, this high voltage is almost invariably full-wave rectified and smoothed DC.

6.1.2.2. *Rotating-anode X-ray tubes*

The sealed tubes described above are convenient and require little maintenance, but their power dissipation, and thus their X-ray output, is limited. For macromolecular crystallography, the most commonly used tubes are continuously pumped, demountable tubes with water-cooled rotating targets [see the reviews by Yoshimatsu & Kozaki (1977) and Phillips (1985)]. At present, these tubes mostly employ ferro-fluidic vacuum shaft seals (Bailey, 1978), which have an operational life of several thousand hours before they need replacement. The need for a beam with a small cross fire calls for a focal spot preferably not larger than 0.15 × 0.15 mm. This is usually achieved by focusing the electrons on the target to a line 0.15 mm wide and 1.5 mm long (in the direction parallel to the rotation axis of the target). The line is then viewed at an angle of 5.7° to give a 10:1 foreshortening. Foci down to this size can be produced on a target mounted close to an electron gun. For smaller focal spots, such as those of the microfocus tube described below, it

Table 6.1.2.1. *Standard X-ray tube inserts*

Focus size on target (mm × mm)	Recommended power loading (kW)
8 × 0.15	0.8
8 × 0.4	1.5
10 × 1.0	2.0
12 × 2.0	2.7

is necessary to employ an electron lens (which may be magnetic or electrostatic) to produce on the target a demagnified image of the electron cross-over, which is close to the grid of the tube cathode.

The maximum power that can be dissipated in the target without damaging the surface has been discussed by Müller (1929, 1931), Oosterkamp (1948), and Ishimura *et al.* (1957). The later calculations are in adequate agreement with Müller's results, from which the power W for a copper target is given by

$$W = 26.4\, f_1 (f_2 \nu)^{1/2}.$$

Here, W is in watts, f_1 and f_2 are the length and the width of the focal line in mm, and ν is the linear speed of the target surface in mm s^{-1}; it is assumed that the surface temperature of the target reaches 600 °C, well below the melting point of copper (1083 °C). Thus, for a focal spot 1.5×0.15 mm and for an 89 mm-diameter target rotating at 6000 revolutions min^{-1} (ν = 28 000 mm s^{-1}), Müller's formula gives a maximum permissible power loading of 2.5 kW or 57 mA at 45 kV. This agrees well with the experimentally determined loading limit.

Green & Cosslett (1968) have made extensive measurements of the efficiency of the production of characteristic radiation for a number of targets and for a range of electron accelerating voltages. Their results have been verified by many subsequent investigators. For a copper target, they found that the number of $K\alpha$ photons emitted per unit solid angle per incident electron is given by

$$N/4\pi = 6.4 \times 10^{-5} [E/E_k - 1]^{1.63},$$

where E is the tube voltage in kV and E_k = 8.9 keV is the K excitation voltage.

Accordingly, the number of $K\alpha$ photons generated per second per steradian per mA of tube current is 1.05×10^{12} at 25 kV and 4.84×10^{12} at 50 kV.

Of the generated photons, only a fraction, usually denoted by $f(\chi)$ (Green, 1963), emerges from the target as a result of X-ray absorption in the target. $f(\chi)$ decreases with increasing tube voltage and with decreasing take-off angle. It has a value of about 0.5 for E = 50 kV and for a take-off angle of 5°.

The X-ray beam is further attenuated by absorption in the tube window (~80% transmission), by the air path between the tube and the sample, and by any β-filters which may be used.

In a typical diffractometer or image-plate arrangement where no beam conditioning other than a β-filter is employed, the sample may be 300 mm from the tube focus and the limiting aperture at that point might have a diameter of 0.3 mm, so that the full-angle cross fire at the sample is 1.0×10^{-3} rad. The solid angle subtended by the limiting aperture at the source is 7.9×10^{-7} steradians. At 50 kV and 60 mA, the X-ray flux through the sample will be approximately 4.5×10^7 photons s^{-1}. These figures are approximately confirmed by unpublished experimental measurements by Arndt & Mancia and by Faruqi & Leslie. It is interesting to note that the power in this photon flux is 5.8×10^{-8} W, which is a fraction of 2×10^{-11} of the power loading of the X-ray tube target.

Instead of simple aperture collimation, one of the types of focusing collimators described in Section 6.1.4.1 below may be used. They collect a somewhat larger solid angle of radiation from the target of a conventional X-ray source than does a simple collimator and some produce a higher intensity at the sample.

6.1.2.3. *Microfocus X-ray tubes*

Standard sealed X-ray tubes with a stationary target deliver a collimated intensity to the sample which is insufficient for most applications in macromolecular crystallography. These tubes have foreshortened foci between 0.4 and 2 mm^2 which do not lend themselves to efficient collimation by means of focusing mirrors or monochromators without introducing a cross fire in the beam that is too large for our purposes.

The situation is different with microfocus tubes, which are discussed in Section 6.1.4.2. Here, a relatively large solid angle of collection can make up for the lower power dissipation which results from the small electron focus.

6.1.2.4. *Synchrotron-radiation sources*

Charged particles with energy E and mass m moving in a circular orbit of radius R at a constant speed ν radiate a power, P, into a solid angle of 4π, where

$$P = 88.47 E^4 I/R,$$

where E is in GeV, I is the circulating electron or positron current in ampères and R is in metres. Thus, for example, in a bending-magnet beam line at the ESRF, Grenoble, France, R = 20 m, and at 5 GeV and 200 mA, P = 554 kW.

For relativistic electrons, the electromagnetic radiation is compressed into a fan-shaped beam tangential to the orbit, with a vertical opening angle $\Psi \simeq mc^2/E$, *i.e.* 0.1 mrad for E = 5 GeV (Fig. 6.1.2.2). This fan rotates with the circulating electrons; if the ring is filled with n bunches of electrons, a stationary observer will see n flashes of radiation every $2\pi R/c$ s, the duration of each flash being less than 1 ns.

The spectral distribution of synchrotron radiation extends from the infrared to the X-ray region; Schwinger (1949) gives the instantaneous power radiated by a monoenergetic electron in a circular motion per unit wavelength interval as a function of wavelength (Winick, 1980). An important parameter specifying the distribution is the critical wavelength, λ_c: half the total power radiated, but only ~9% of the total number of photons, is at $\lambda < \lambda_c$ (Fig. 6.1.2.6). λ_c (in Å) is given by

$$\lambda_c = 18.64/(BE^2),$$

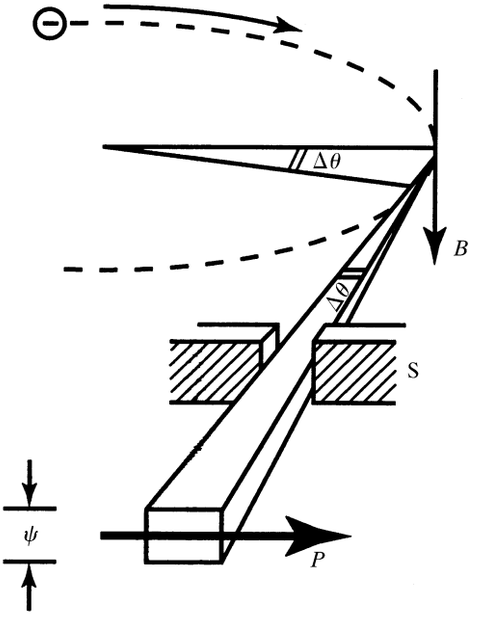

Fig. 6.1.2.2. Synchrotron radiation emitted by a relativistic electron travelling in a curved trajectory. B is the magnetic field perpendicular to the plane of the electron orbit; ψ is the natural opening angle in the vertical plane; P is the direction of polarization. The slit, S, defines the length of the arc of angle, $\Delta\theta$, from which the radiation is taken. From Buras & Tazzari (1984).

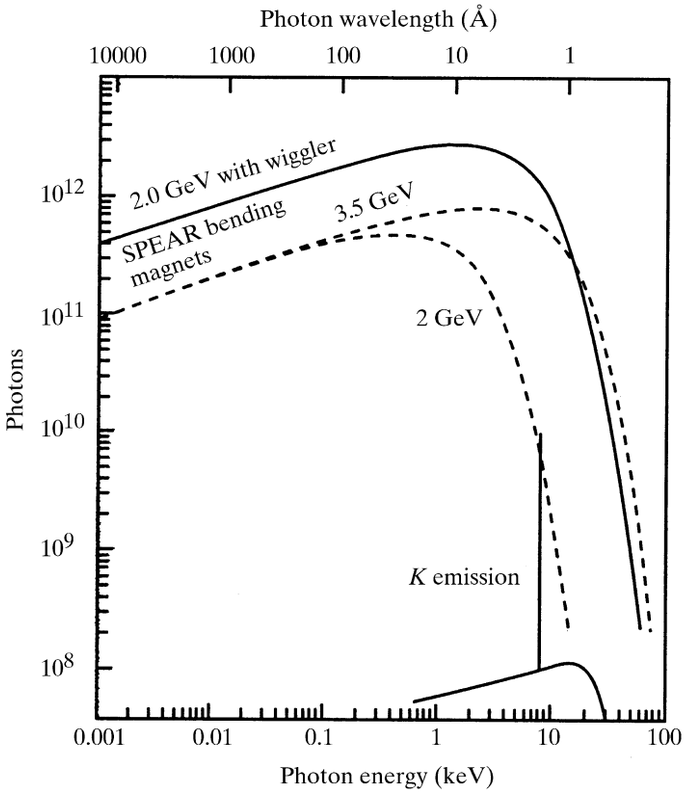

Fig. 6.1.2.3. Comparison of the spectra from the storage ring SPEAR in photons s^{-1} mA^{-1} $mrad^{-1}$ per 1% band pass (1978 performance) and a rotating-anode X-ray generator, showing the Cu *K* emission line and the *Bremsstrahlung*. Reproduced with permission from Nagel (1980). Copyright (1980) New York Academy of Sciences.

where B $(= 3.34E/R)$ is the magnetic bending field in T, E is in GeV and R is in metres.

The orbit of the particle can be maintained only if the energy lost, in the form of electromagnetic radiation, is constantly replenished. In an electron synchrotron or in a storage ring, the circulating particles are electrons or positrons maintained in a closed orbit by a magnetic field; their energy is supplied or restored by means of an oscillating radiofrequency (RF) electric field at one or more places in the orbit. In a synchrotron designed for nuclear-physics experiments, the circulating particles are injected from a linear accelerator, accelerated up to full energy by the RF field, and then deflected onto a target with a cycle frequency of about 50 Hz. The synchrotron radiation is thus produced in the form of pulses of this

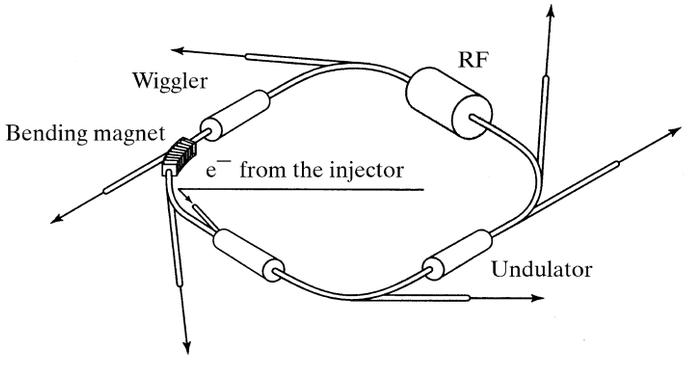

Fig. 6.1.2.4. Main components of a dedicated electron storage-ring synchrotron-radiation source. For clarity, only one bending magnet is shown. From Buras & Tazzari (1984).

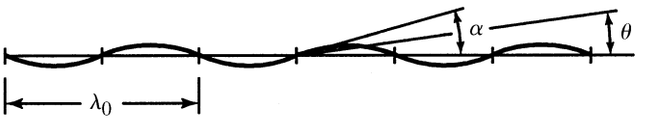

Fig. 6.1.2.5. Electron trajectory within a multipole wiggler or undulator. λ_0 is the spatial period, α is the maximum deflection angle and θ is the observation angle. From Buras & Tazzari (1984).

frequency. A storage ring, on the other hand, is filled with electrons or positrons, and after acceleration the particle energy is maintained by the RF field; ideally, the current circulates for many hours and decays only as a result of collisions with remaining gas molecules. At present, only storage rings are used as sources of synchrotron radiation, and many of these are dedicated entirely to the production of radiation: they are not used at all, or are used only for limited periods, for nuclear-physics collision experiments.

Synchrotron radiation is highly polarized. In an ideal ring, where all electrons are parallel to one another in a central orbit, the radiation in the orbital plane is linearly polarized with the electric vector lying in this plane. Outside the plane, the radiation is elliptically polarized.

In practice, the electron path in a storage ring is not a circle. The 'ring' consists of an alternation of straight sections and bending magnets. Beam lines are installed at the bending magnets and at the insertion devices.

These insertion devices with a zero magnetic field integral, *i.e.* wigglers and undulators, may be inserted in the straight sections (Fig. 6.1.2.4). A wiggler consists of one or more dipole magnets with alternating magnetic field directions aligned transverse to the orbit. The critical wavelength can thus be shifted towards shorter values because the bending radius can be decreased over a short section, especially when superconducting magnets are used. Such a device is called a wavelength shifter. If it has N dipoles, the radiation from the different poles is added to give an N-fold increase in intensity. Wigglers can be horizontal or vertical. In a wiggler, the maximum divergence, 2α, of the electron beam is much larger than ψ, the vertical aperture of the radiation cone in the spectral region of interest (Fig. 6.1.2.2). If $2\alpha \ll \psi$, and if, in addition, the magnet poles of a multipole device have a short period, then the device becomes an undulator; interference takes place between the radiation of wavelength λ_0 emitted at two points λ_0 apart on the electron trajectory (Fig. 6.1.2.5). The spectrum at an angle θ to the axis observed through a pinhole consists of a single spectral line and its harmonics with wavelengths

$$\lambda_i = i^{-1}\lambda_0[(E/mc^2)^{-2} + \alpha^2/2 + \theta^2]/2$$

(Hofmann, 1978). Typically, the bandwidth of the lines, $\delta\lambda/\lambda$, is $\sim$0.01 to 0.1, and the photon flux per unit bandwidth from the undulator is many orders of magnitude greater than that from a bending magnet. Undulators at the ESRF have a fundamental wavelength of less than 1 Å.

The spectra for a bending magnet and a wiggler are compared with that from a copper-target rotating-anode tube in Fig. 6.1.2.3.

6.1.3. Properties of the X-ray beam

We must now consider the properties of the X-ray beam necessary for the gathering of intensity data from single crystals of biological macromolecules. The properties of the beam with which we are concerned are:

(*a*) the size of the beam appropriate for the sample dimensions;
(*b*) the X-ray wavelength and its spectral purity;
(*c*) the intensity in photons s^{-1};

(*d*) the cross fire, that is, the maximum angle between rays in the beam;

(*e*) the temporal structure of the beam, that is, its stability or constancy, and for generators other than X-ray tubes, the duration and frequency of intensity pulses.

These properties cannot be considered in isolation since the requirements depend on the particular crystal under investigation (size, unit-cell dimensions, mosaic spread and resistance to radiation damage), on the geometry of the X-ray camera or diffractometer and on the detector used.

6.1.3.1. *Beam size*

The best signal-to-noise ratio in the diffraction pattern is secured when the sample crystal is just bathed in the X-ray beam, which is often taken to be about 0.2 to 0.3 mm in diameter. Unfortunately, many crystals are plate- or needle-shaped and present a greatly varying aspect to the beam. To date, no-one has described data-collection instruments in which the incident-beam dimension is changed automatically as the crystal is rotated; the next best thing is a versatile collimation system that makes use of interchangeable beam-limiting apertures.

6.1.3.2. *X-ray wavelength*

For X-ray tube sources, the main component of the beam is the characteristic radiation of the tube target. The vast majority of macromolecular structure determinations have been carried out with copper $K\alpha$ X-rays of wavelength 1.54 Å. These are reasonably well matched to the linear absorption coefficients of biological materials. Diffractometers and cameras are usually designed to permit data collection out to Bragg angles of about 30°, that is, to a minimum spacing of 1.54 Å, which is a convenient limit.

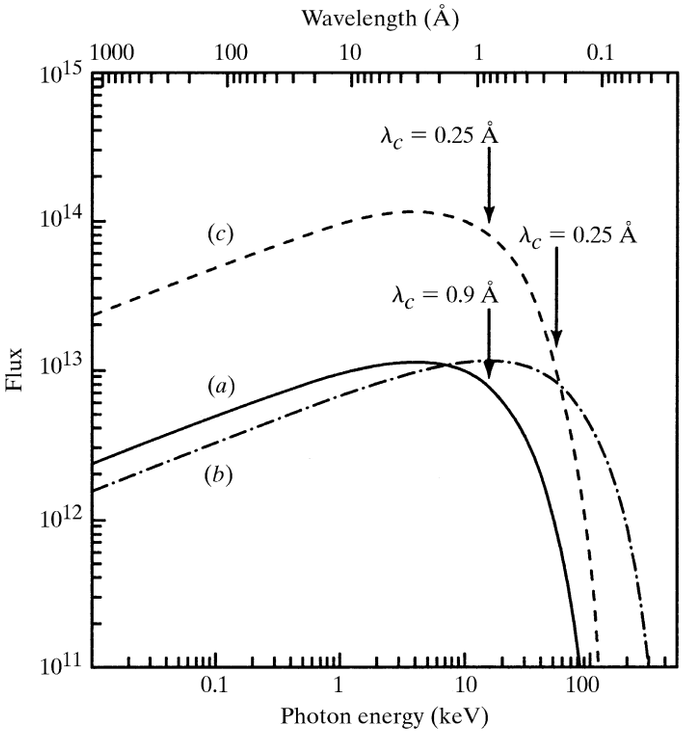

Fig. 6.1.2.6. Spectral distribution and critical wavelengths for (*a*) a dipole magnet, (*b*) a wavelength shifter and (*c*) a multipole wiggler at the ESRF. From Buras & Tazzari (1984).

The next shortest, useful characteristic X-rays are, in practice, those from a molybdenum target (0.71 Å), but are rarely used in macromolecular crystallography.

The advantages of shorter wavelengths are a reduced absorption correction, smaller angles of incidence on the film, image plate or area detector, and, probably, a slightly smaller amount of radiation damage for a given intensity of the diffraction pattern. The disadvantage is a lower diffracted intensity, which is approximately proportional to the square of the wavelength. Crystal monochromators and specularly reflecting X-ray mirrors have a lower reflectivity for shorter wavelengths; most X-ray detectors, other than image plates and scintillation counters, are less efficient for harder X-rays (see Part 7).

At synchrotron beam lines where there is no shortage of X-ray intensity, it is now customary to select X-ray wavelengths of about 1 Å for routine data collection. Here, of course, it is possible to choose optimum wavelengths for anomalous-dispersion phasing experiments. This possibility is one of the major advantages of synchrotron radiation. The selection of a narrow wavelength band from the white radiation continuum (*Bremsstrahlung*) of an X-ray tube by means of crystal monochromators is not of practical importance: a tungsten-target X-ray tube operated at 80 kV produces about 1×10^{-5} 8 keV photons per steradian per electron incident on the target within a wavelength band, $\delta\lambda/\lambda$, of 10^{-3}; a copper-target X-ray tube at 40 kV produces about 5×10^{-4} $K\alpha$ photons per steradian per electron, that is, about 50 times more X-rays.

6.1.3.3. *Spectral composition*

Any X-rays outside the wavelength band used for generating the desired X-ray pattern contribute to the radiation damage of the sample and to the X-ray background. In the interests of resolving neighbouring diffraction spots in the pattern, one would require the wavelength spread, $\delta\lambda/\lambda$, in the incident radiation to be less than 5×10^{-3}. For the Cu $K\alpha$ doublet $(\lambda_{\alpha_2} - \lambda_{\alpha_1})/\lambda \simeq 2.5 \times 10^{-3}$ and the doublet nature of the line usually does not matter. On the other hand, the value of $(\lambda_\alpha - \lambda_\beta)/\lambda$ is 0.1, so the $K\beta$ component must be eliminated by means of a β-filter (a 0.15 mm-thick nickel foil for copper radiation) or by reflection from a crystal monochromator to avoid the appearance of separate $K\beta$ diffraction spots. The dispersion produced by a crystal monochromator is small enough to be ignored in most applications.

In synchrotron beam lines, the bandpass is usually determined by the divergence of the beam and is of the order of 10^{-4}. This is a smaller bandpass than is required for most purposes, and intensity can be gained by widening the bandpass by the use of an asymmetric-cut monochromator in spatial expansion geometry (Nave *et al.*, 1995; Kohra *et al.*, 1978). The intensity outside the monochromator bandpass is usually totally negligible.

6.1.3.4. *Intensity*

The intensity of the primary X-ray beam should be such as to allow data collection in a reasonably short time; increased speed is one of the main factors which has led to the popularity of synchrotron-radiation data collection as compared to data collection using conventional sources. Moreover, the radiation damage to the sample per unit incident dose is smaller at high intensities. This does not mean that ever more intense beams are necessary for today's protein-crystallography problems; very often, the speed of data collection is limited by the read-out time of the detector; the counting-rate capabilities of present-day X-ray detectors make it impossible to use in full the intensities available at some beam lines. With the widespread use of cryocrystallographic methods (Part 10), radiation damage is no longer as severe a problem as it once was.

No doubt, the day will come when available intensities will be so high that instantaneous structure determination will become a possibility, but this will require major advances in X-ray detectors, probably in the form of the development of large pixel detectors (*e.g.* Beuville *et al.*, 1997).

There is still some scope for increasing the intensity of X-ray beams from conventional sources, which offer the advantage of making measurements in the local laboratory instead of at some remote central facility.

6.1.3.5. *Cross fire*

The cross fire is defined as the angle or the half-angle between extreme rays in the beam incident on a given point of the sample. In the absence of focusing elements, such as specularly reflecting mirrors, the X-ray beam diverges from the source. A diverging beam can be turned into a converging one by reflection from a curved mirror or crystal. A crystal with constant lattice spacing can change the sign, but not the magnitude, of the angle between rays, whatever the curvature of the crystal; the deviation produced by a reflection anywhere on the surface of the crystal must always be twice the Bragg angle. It is possible to change a divergent beam into a convergent one with a different cross fire by specular reflection at a mirror or by means of a crystal in which the lattice spacing varies from point to point along the length of the plate. Such variable-spacing reflectors may be either artificial-crystal multilayers (Schuster & Göbel, 1997) or, less commonly, natural crystals whose spacing is modified by variable doping or by a temperature gradient along the crystal plate (Smither, 1982). In the neutron-scattering community, graded-spacing multilayer monochromators are usually referred to as 'supermirrors' (see Section 6.2.1.3.3 in Chapter 6.2).

The construction of curved mirrors and curved-crystal monochromators is discussed below.

As a general rule, the better the collimation of the incident X-ray beam, that is, the smaller the cross fire and the more nearly parallel the beam, the cleaner the diffraction pattern and the lower the background. Synchrotron-radiation sources permit a certain prodigality in X-ray intensity and the beams from them are thus usually better collimated than beams from conventional sources.

The useful degree of collimation depends on the crystal under investigation. The aim in the design of an instrument for data collection from single crystals must be to make the widths of the angular profiles of the reflection small, but these widths cannot be reduced beyond the rocking-curve width determined by the mosaic spread of the sample, however small the cross fire. The mosaic spread of a typical protein crystal is often quoted as being about 10^{-3} rad or about 3.4 minutes of arc. However, there are many crystals with much larger mosaicities; for such samples, the intensity of the X-ray beam, expressed as the total number of photons which strike the crystal, can be increased by permitting a larger cross fire.

The mosaic spread must be understood as the angle between individual domains of the mosaic crystal. These domains may be as large as 100 μm, that is, they may have dimensions not so very much smaller than those of the macroscopic crystal. The individual rocking-curve widths may be as small as 10 seconds of arc (50 μrad). Fourme *et al.* (1995) have discussed the implications of this degree of perfection if the collimation is improved to a stage where it can be exploited.

The way in which the cross fire influences the angular widths of the reflections depends on the instrument geometry. In a single-counter four-circle diffractometer, all reflections are brought onto the equator and the crystal is rotated about an axis perpendicular to the equatorial plane. The cross fire should, therefore, be small parallel to the equatorial plane, *i.e.* usually in the horizontal plane. The cross fire in the plane containing the rotation axis affects the angular width of the reflections much less, and it could thus be made larger in the interest of a high intensity.

The situation is different if the diffractometer is fitted with an electronic area detector, such as a CCD or other TV detector or a multi-wire proportional chamber (see Part 7). Here, the widths of reflections in upper levels are affected by the cross fire in the plane containing the crystal rotation axis, and the divergence or convergence of the beam in this plane should also be kept small.

With recording on photographic film or image plates, each exposure, or 'shot' or 'frame', corresponds to a crystal rotation that is usually many times larger than the angular width of a reflection. It is then less important to keep the cross fire small in the plane perpendicular to the rotation axis of the crystal.

In many collimation arrangements, the cross fire can be chosen independently in the two planes. In the absence of monochromators or mirrors, the cross fire is determined by beam apertures, which can be rectangular slits; it is, of course, simpler to employ circular holes, which give the same cross fire in both planes.

6.1.3.6. *Beam stability*

The synchrotron beam decays steadily after each filling of the ring as the number of stored positrons or electrons decays. Even with an X-ray tube operated from voltage- and current-stabilized supplies, the X-ray intensity changes with time as a result of contamination and roughening of the target surface. It is, thus, highly desirable to have a method of monitoring the beam incident on the sample, for example, by means of an ionization chamber built into the collimator (Arndt & Stubbings, 1988).

It should be noted that when the collimator contains focusing elements, the intensity at the sample can vary by several hundred per cent, depending on the exact alignment of the focusing mirrors or crystals and on the exact dimensions of the electron focus on the tube target.

Intensity changes can be caused by mechanical movement of collimating components. Among these may be such unsuspected effects as flexing of the target surface with changes in cooling-water pressure.

The response of an incident-beam monitor may itself vary as a result of changes in temperature, barometric pressure, or humidity.

Synchrotron radiation from storage rings has a regular time-dependent modulation brought about by the rate of passage of bunches of electrons or positrons in the ring. For the great majority of measurements, this time structure has no effect, but at very high intensities, the counting losses are greater than they would be from a steady source.

6.1.4. Beam conditioning

The primary X-ray beam from the source is conditioned by a variety of devices, such as filters, mirrors and monochromators, to produce the appropriate properties for the beam incident on the sample.

6.1.4.1. *X-ray mirrors*

It is usually necessary to focus the X-ray beam in two orthogonal directions. This can be achieved either by means of one mirror with curvatures in two orthogonal planes or by two successive reflections from two mirrors which are curved in one plane and planar in the other; the two planes of curvature must be at right angles to one another. In the arrangement adopted by Kirkpatrick & Baez (1948) and by Franks (1955), the two mirrors lie one behind the other (Fig. 6.1.4.1) and thus produce a different degree of collimation in the two planes. Instead of this tandem arrangement, the mirrors can lie side-by-side, as proposed by Montel (1957), to form what the author

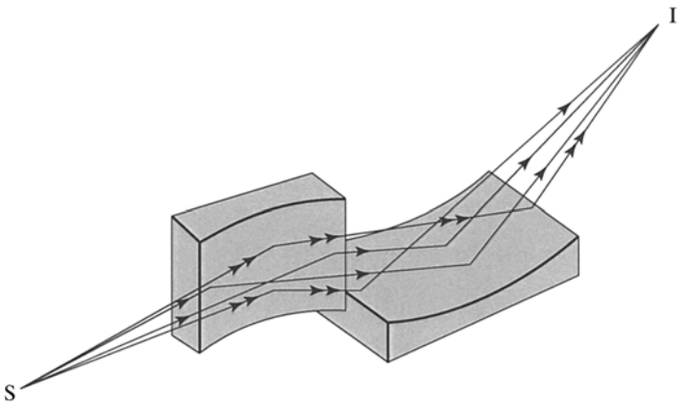

Fig. 6.1.4.1. Production of a point focus by successive reflections at two orthogonal curved mirrors. Arrangement due to Kirkpatrick & Baez (1948) and to Franks (1955).

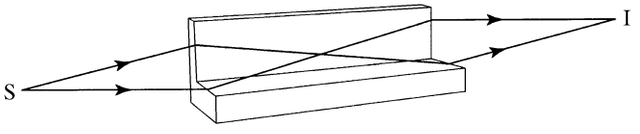

Fig. 6.1.4.2. The 'catamegonic' arrangement of Montel (1957), in which two confocal mirrors with orthogonal curvatures lie side-by-side.

calls a 'catamegonic roof' (Fig. 6.1.4.2). The mirrors are then best made from thicker material, and the reflecting surfaces are ground to the appropriate curvature. The same arrangement has been used by Osmic Inc. (1998) for their Confocal Max-Flux Optics, in which the curved surfaces are coated with graded-spacing multilayers.

Flat mirror plates can be bent elastically to a desired curvature by applying appropriate couples. Fig. 6.1.4.3 shows the bending method adopted by Franks (1955). A cylindrical curvature results from a symmetrical arrangement that produces equal couples at both ends. With appropriate unequal couples applied at the two ends of the plate, the curvature can be made parabolic or elliptical. Precision elliptical mirrors have been produced by Padmore *et al.*

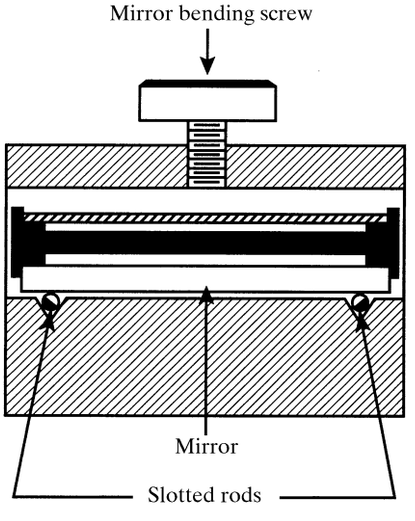

Fig. 6.1.4.3. Mirror bender (after Franks, 1955). The force exerted by the screw produces two equal couples which bend the mirror into a circular arc. The slotted rods act as pivots and also as beam-defining slits.

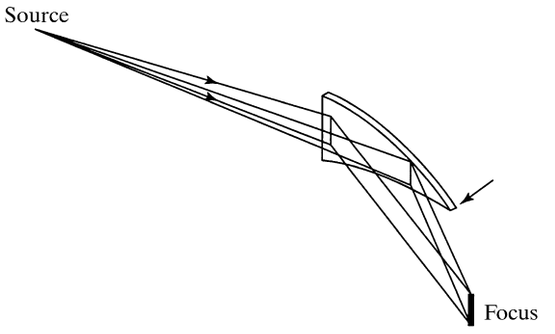

Fig. 6.1.4.4. Triangular mirror bender as described by Lemonnier *et al.* (1978) for crystal plates and by Milch (1983) for glass mirrors. The base of the triangular plate is clamped and the bending force is applied at the apex along the arrow.

(1997); unequal couples are applied in this way. Cylindrically curved mirrors can be produced by applying a force at the tip of a triangular plate whose base is firmly anchored (Fig. 6.1.4.4). Lemonnier *et al.* (1978) first used this method for making curved-crystal monochromators. Milch (1983) described X-ray mirrors made in this way; the effect of the linear increase of the bending moment along the plate is compensated by the linear increase of the plate section so that the curvature is constant. An elliptical or a parabolic curvature results if either the width or the thickness of the plate is made to vary in an appropriate way along the length of the plate. Arndt, Long & Duncumb (1998) described a monolithic mirror-bending block in which the mirror plates are inserted into slots cut to an elliptical curvature by ion-beam machining. The solid angle of collection is made four times larger than for a two-mirror arrangement by providing a pair of horizontal mirrors and a pair of vertical mirrors in tandem in one block (Fig. 6.1.4.5).

Mirror plates for these benders are usually made from highly polished glass, quartz, or silicon plates which are coated with nickel, gold, or iridium.

Mirrors for synchrotron beam lines that focus the radiation in the vertical plane are most often ground and polished to the correct shape, rather than bent elastically. Much longer mirrors can be made in this way.

The collecting efficiency of specularly reflecting mirrors depends on the reflectivity of the surface and on the solid angle of collection; this, in turn, is a function of the maximum glancing angle of incidence, which is the critical angle for total external reflection, θ_c.

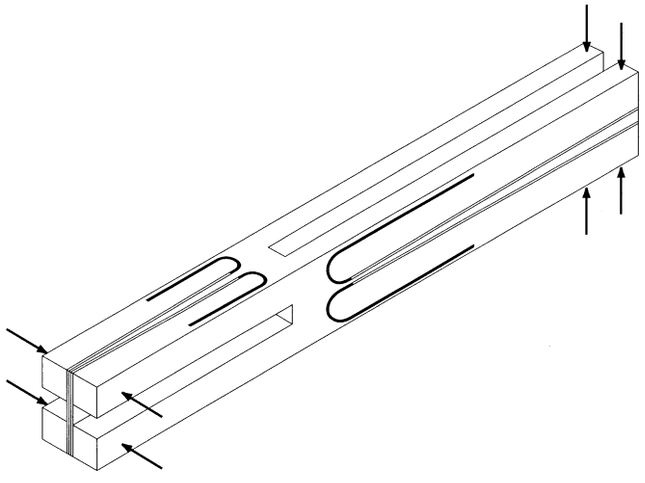

Fig. 6.1.4.5. Mirror holder with machined slots for two orthogonal pairs of curved mirrors (after Arndt, Duncumb *et al.*, 1998).

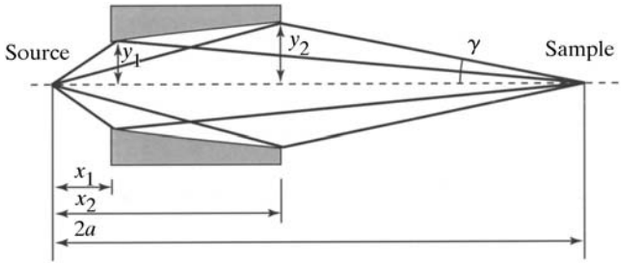

Fig. 6.1.4.6. Ellipsoidal mirror for use with a microfocus X-ray tube, where x_1 is ∼15 mm. The major axis, $2a$, may be up to 600 mm, whereas the exit aperture, $2y_2$, lies in the region 0.8–1.4 mm. The angle γ determines the cross fire on the sample and is less than 1 rad.

For X-rays of wavelength λ, measured in Å,

$$\theta_c \simeq 2.32 \times 10^{-3}(Z\rho/A)^{1/2}\lambda,$$

where Z is the atomic number, A is the atomic mass and ρ is the specific gravity of the reflecting surface.

Thus, for Cu $K\alpha$ radiation and a gold surface, $\theta_c \simeq 10$ mrad. The reflectivity of the mirror surface is strongly dependent on the surface roughness; for the reflectivity to be more than 50%, the r.m.s. roughness must not exceed 10 Å.

It is not possible to design a reflecting collimator with a planar angle of collection greater than about $3\theta_c$. For the shorter wavelengths, in particular, variable-spacing multilayer mirrors (Schuster & Göbel, 1997) hold considerable promise. If the spacing at the upstream end of the mirror is 30 Å, the largest angles of incidence will be 26 and 17 mrad for 1.54 and 1.0 Å X-rays, respectively. By comparison, the critical angles at a gold surface for these radiations are 10 and 6.5 mrad, respectively.

6.1.4.2. *Focusing collimators for microfocus sources*

In most arrangements that include conventional X-ray tubes, the planar angle of collection is very small. A more efficient use is always made of the radiation from the target by a focusing collimator, which forms an image of the source on the sample (Fig. 6.1.4.6). The angle of collection should be as large as possible, while the cross fire, *i.e.* the angle of convergence, is kept small, say, at about 10^{-3} rad. It is possible to design focusing collimators based on gold-surfaced toroids of revolution (Elliott, 1965), which afford a planar angle of collection of about three times the critical angle for total external reflection, that is, about 30×10^{-3} rad.

Consequently, the mirror should *magnify* about 30 times, and if the image diameter, determined by a typical sample size, is to be 300 µm, the size of the focus should be about 10 µm. The solid angle of collection of such an imaging toroid is about 8×10^{-4} steradians, that is, more than 1000 times greater than the solid angle of a simple non-imaging collimator. The averaged mirror reflectivity achieved at present is about 0.3, so the microfocus tube and toroidal mirror combination produces a similar intensity at the sample as the conventional tube with a non-focusing collimator at about 300 times the power. Future increases of the reflectivity are likely as the surface roughness of the mirrors is improved.

A suitable microfocus tube has been described by Arndt, Long & Duncumb (1998); mirrors used with this tube were discussed by Arndt, Duncumb *et al.* (1998). The tube design allows the distance between the source and the mirror to be as little as 10 mm in order to achieve the necessary magnification without making the distance between the tube and the sample inconveniently long.

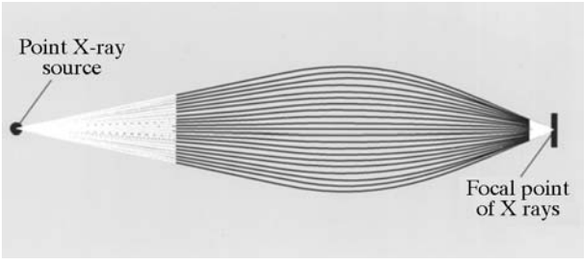

Fig. 6.1.4.7. A polycapillary collimator (after Bly & Gibson, 1996).

6.1.4.3. *Other focusing collimators*

There has been very active development in recent years of tapering capillaries for focusing X-rays, either as individual capillaries (see the review by Bilderback *et al.*, 1994), or in the form of multicapillary bundles. The latter were first described by Kumakhov & Komarov (1990); since then, they have undergone great improvements in the form of fused bundles (Bly & Gibson, 1996) (Fig. 6.1.4.7). Single capillaries have found the greatest use as X-ray concentrators, where a larger-diameter beam of X-rays enters the large end of a tapered capillary and is concentrated to a diameter of a few µm. Fused polycapillary bundles have been employed as focusing collimators for protein crystallography (MacDonald *et al.*, 1999). Both types of capillary optics are usually designed as multi-bounce devices, in which the X-rays undergo several, or many, reflections at the walls of the capillary; consequently the cross-fire half-angle at the output end has a value about equal to the critical angle for reflection at a glass surface or, perhaps, 4 mrad. This is sometimes too great for producing diffraction patterns with an optimum signal-to-background ratio.

Other methods of focusing X-rays, such as zone plates (Kirz, 1974) and refractive optics, are being investigated, but at present none of them can compare with toroidal reflectors for data collection from single crystals of macromolecules.

6.1.4.4. *Crystal monochromators*

When the X-rays from the tube target are specularly reflected by a mirror, the spectrum is cut off for X-rays below the shortest wavelength for which the critical angle is equal to the smallest angle of incidence on the mirror. For a typical mirror designed for Cu $K\alpha$ radiation, this cutoff wavelength might be about 0.75 Å, and the harder X-rays can be further attenuated by a β-filter. Of course, the more nearly monochromatic the radiation falling on the sample, the lower the radiation damage and the higher the spot-to-background ratio in the recorded patterns.

White radiation is almost completely eliminated by reflecting the primary X-ray beam using a natural or artificial (multilayer) crystal. The most commonly used type of plane monochromator for macromolecular crystallography is a single crystal of graphite. This material (HOPG, or highly ordered pyrolytic graphite) has a relatively large mosaic spread, typically about 0.4°, and it cannot separate the $K\alpha$ doublet. This separation is essential in most small-molecule investigations, but is unnecessary for macromolecular crystals, which rarely diffract beyond 1.5 Å, and disadvantageous where a high intensity of the beam reflected by the monochromator is the main consideration.

The intensity of the diffraction pattern obtained with a graphite monochromator is only about two or three times lower than that resulting from a β-filtered pinhole-collimated beam. The situation is different at synchrotron beam lines, which must incorporate a monochromator in order to select the desired X-ray energy band. Curved focusing crystals collect X-rays over a relatively large horizontal angular range and thus produce a beam with a horizontal

convergence angle of up to several milliradians. Much more nearly parallel beams are produced by reflection at several crystals in tandem, often in the form of monolithic channel-cut monochromators. In present-day storage rings, the power density at the first optical element is of the order of $10\,\mathrm{W\,mm^{-2}}$ at wiggler and undulator beam lines. This amount of power can be dissipated by careful design of water-cooling channels (Quintana & Hart, 1995; van Silfhout, 1998). In addition, the monochromator crystal, usually of silicon or germanium, may be profiled to minimize distortions as a result of thermal stresses.

The next generation of insertion devices will subject the optical elements to loads of several hundred $\mathrm{W\,mm^{-2}}$. Possible engineering solutions to the very severe heat-loading problem include the use of diamond crystals as reflecting elements. This material has a very high thermal conductivity, especially at low temperatures.

References

6.1

Arndt, U. W., Duncumb, P., Long, J. V. P., Pina, L. & Inneman, A. (1998). *Focusing mirrors for use with microfocus X-ray tubes. J. Appl. Cryst.* **31**, 733.

Arndt, U. W., Long, J. V. P. & Duncumb, P. (1998). *A microfocus X-ray tube used with focusing collimators. J. Appl. Cryst.* **31**, 936–944.

Arndt, U. W. & Stubbings, S. J. (1988). *Miniature ionisation chambers. J. Appl. Cryst.* **21**, 577.

Bailey, R. L. (1978). *The design and operation of magnetic liquid shaft seals.* In *Thermomechanics of magnetic fluids*, edited by B. Berkovsky. London: Hemisphere.

Beuville, E., Beche, J.-F., Cork, C., Douence, V., Earnest, J., Millaud, D., Nygren, H., Padmore, B., Turko, G., Zizka, G., Datte, P. & Xuong Ng, H. (1997). *Two-dimensional pixel array sensor for protein crystallography. Proc. SPIE*, **2859**, 85–92.

Bilderback, D. H., Thiel, D. J., Pahl, R. & Brister, K. E. (1994). *X-ray applications with glass-capillary optics. J. Synchrotron Rad.* **1**, 37–42.

Bly, P. & Gibson, D. (1996). *Polycapillary optics focus and collimate X-rays. Laser Focus World*, March issue.

Buras, B. & Tazzari, S. (1984). Editors. *European Synchrotron Radiation Facility.* Geneva: ESRP.

Elliott, A. (1965). *The use of toroidal reflecting surfaces in X-ray diffraction cameras. J. Sci. Instrum.* **42**, 312–316.

Forsyth, J. M. & Frankel, R. D. (1984). *Experimental facility for nanosecond time-resolved low-angle X-ray diffraction experiments using a laser-produced plasma source. Rev. Sci. Instrum.* **55**, 1235–1242.

Fourme, R., Ducruix, A., Ries-Kautt, M. & Capelle, B. (1995). *The perfection of protein crystals probed by direct recording of Bragg reflection profiles with a quasi-planar X-ray wave. J. Synchrotron Rad.* **2**, 136–142.

Franks, A. (1995). *An optically focusing X-ray diffraction camera. Proc. Phys. Soc. London Sect. B*, **68**, 1054–1069.

Genz, H., Graf, H.-D., Hoffmann, P., Lotz, W., Nething, U., Richter, A., Kohl, H., Weickenmeyer, A., Knüpfer, W. & Sellschop, J. P. F. (1990). *High intensity electron channeling and perspectives for a bright tunable X-ray source. Appl. Phys. Lett.* **57**, 2956–2958.

Green, M. (1963). *The target absorption correction in X-ray microanalysis.* In *X-ray optics and X-ray microanalysis*, edited by H. H. Pattee, V. E. Cosslett & A. Engström, pp. 361–377. New York and London: Academic Press.

Green, M. & Cosslett, V. E. (1968). *Measurements of K, L and M shell X-ray production efficiencies. Br. J. Appl. Phys. Ser.* 2, **1**, 425–436.

Hofmann, A. (1978). *Quasi-monochromatic synchrotron radiation from undulators. Nucl. Instrum. Methods*, **152**, 17–21.

International Tables for Crystallography (1999). Vol. C. *Mathematical, physical and chemical tables*, edited by A. J. C. Wilson & E. Prince. Dordrecht: Kluwer Academic Publishers.

Ishimura, T., Shiraiwa, Y. & Sawada, M. (1957). *The input power limit of the cylindrical rotating anode of an X-ray tube. J. Phys. Soc. Jpn*, **12**, 1064–1070.

Kirkpatrick, P. & Baez, A. V. (1948). *J. Opt. Soc. Am.* **56**, 1–13.

Kirz, J. (1974). *Phase zone plates for X-rays and the extreme UV. J. Opt. Soc. Am.* **64**, 301–309.

Kleffer, J. C., Chaker, M., Matte, J. P., Pépin, H., Côté, C. Y., Beaudouin, Y., Johnston, T. W., Chien, C. Y., Coe, S., Mourou, G. & Peyrusse, O. (1993). *Ultra-fast X-ray sources. Phys. Fluids*, **B5**, 2676–2681.

Kohra, K., Ando, M., Natsushita, T. & Hashizume, H. (1978). *Nucl. Instrum. Methods*, **152**, 161–166.

Kumakhov, M. A. & Komarov, F. K. (1990). *Phys. Rep.* **191**, 289–350.

Lemonnier, M., Fourme, R., Rousseaux, F. & Kahn, R. (1978). *X-ray curved-crystal monochromator system at the storage ring DCI. Nucl. Instrum. Methods*, **152**, 173–177.

MacDonald, C. A., Owens, S. M. & Gibson, W. M. (1999). *Polycapillary X-ray optics for microdiffraction. J. Appl. Cryst.* **32**, 160–167.

Milch, J. R. (1983). *A focusing X-ray camera for recording low-angle diffraction from small specimens. J. Appl. Cryst.* **16**, 198–203.

Montel, M. (1957). *X-ray microscopy with catamegonic roof mirrors.* In *X-ray microscopy and microradiography*, edited by V. E. Cosslett, A. Engstrom & H. H. Pattee Jr, pp. 177–185. New York: Academic Press.

Müller, A. (1929). *A spinning target X-ray generator and its input limit. Proc. R. Soc. London Ser. A*, **125**, 507–516.

Müller, A. (1931). *Further estimates of the input limits of X-ray generators. Proc. R. Soc. London Ser. A*, **132**, 646–649.

Nagel, D. J. (1980). *Comparison of X-ray sources. Ann. N. Y. Acad. Sci.* **342**, 235–247.

Nave, C., Clark, G., Gonzalez, A., McSweeney, S., Hart, M. & Cummings, S. (1995). *Tests of an asymmetric monochromator to provide increased flux on a synchrotron radiation beam line. J. Synchrotron Rad.* **2**, 292–295.

Oosterkamp, W. J. (1948). *The heat dissipation in the anode of an X-ray tube. Philips Res. Rep.* **3**, 49–59, 161–173, 303–317.

Osmic Inc. (1998). Sales literature. Osmic Inc., Troy, Michigan, USA.

Padmore, H. A., Ackermann, G., Celestre, R., Chang, C. H., Franck, K., Howells, M., Hussain, Z., Irick, S., Locklin, S., MacDowell, A. A., Patel, J. R., Rah, S. Y., Renner, T. R. & Sandler, R. (1997). *Submicron white-beam focusing using elliptically bent mirrors. Synchrotron Radiat. News*, **10**, 18–26.

Phillips, W. C. (1985). *X-ray sources. Methods Enzymol.* **114**, 300–316.

Piestrup, M. A., Boyers, D. G., Pincus, C. I., Harris, J. L., Maruyama, X. K., Bergstrom, J. C., Caplan, H. S., Silzer, R. M. & Skopik, D. M. (1991). *Quasimonochromatic X-ray source using photo-absorption-edge transition radiation. Phys. Rev. A*, **43**, 3653–3661.

Quintana, J. P. & Hart, M. (1995). *Adaptive silicon monochromators for high-power wigglers; design, finite-element analysis and laboratory tests. J. Synchrotron Rad.* **2**, 119–123.

Schuster, M. & Göbel, H. (1997). *Application of graded multi-layer optics in X-ray diffraction. Adv. X-ray Anal.* **39**, 57–71.

Schwinger, J. (1949). *On the classical radiation of accelerated electrons. Phys. Rev.* **75**, 1912–1925.

Silfhout, R. G. van (1998). *A new water-cooled monochromator at DORIS III. Synchrotron Radiat. News*, **11**, 11–13.

Smither, R. K. (1982). *New methods for focusing X-rays and gamma rays. Rev. Sci. Instrum.* **53**, 131–141.

Winick, H. (1980). *Properties of synchrotron radiation.* In *Synchrotron radiation research*, edited by H. Winick & S. Doniach. New York: Plenum.

Yoshimatsu, M. & Kozaki, S. (1977). *High brilliance X-ray source.* In *X-ray optics*, edited by H.-J. Queisser, ch. 2. Berlin: Springer.

6.2

Ageron, P. (1989). *Cold neutron sources at ILL. Nucl. Instrum. Methods A*, **284**, 197–199.

Akcasu, A. Z., Lellouche, G. S. & Shotkin, L. M. (1971). *Mathematical methods in nuclear reactor dynamics.* New York: Academic Press.

Alberi, J., Fischer, J., Radeka, V., Rogers, L. C. & Schoenborn, B. P. (1975). *A two-dimensional position-sensitive detector for thermal neutrons. Nucl. Instrum. Methods*, **127**, 507–523.

Alsmiller, R. G. & Lillie, R. A. (1992). *Design calculations for the ANS cold source. Part II. Heating rates. Nucl. Instrum. Methods A*, **321**, 265–270.

Bacon, G. E. (1962). *Neutron diffraction.* Oxford University Press.

Böni, P. (1997). *Supermirror-based beam devices. Physica B*, **234–236**, 1038–1043.